

CNTs端鑲埋合金的奈米製程與各製程步驟之結構性質分析

研究生:邱國銘

指導教授:郭正次

國立交通大學
材料科學與工程研究所

中文摘要

為了達成將相變化合金鑲埋於開口端碳奈米管 (carbon nanotubes, CNTs)的頂部孔洞作為奈米解析度儲存媒體之用，首先，以氫氣與甲烷為氣源，由電子迴旋共振化學氣相沉積法，以鈷觸媒輔助成長CNTs。之後，將剛成長出的CNTs在氫電漿環境中作後處理，可將覆蓋觸媒的碳層去除，緊接著浸泡在0.25 M的硝酸溶液中，則頂端的觸媒可被移除。擁有碗狀頂部的開口端CNTs接著以濺鍍製程，被覆蓋一層200 nm的 $\text{Ge}_2\text{Sb}_2\text{Te}_5$ 相變化合金，之後再於真空中熱處理30分鐘，可將CNTs管壁周圍的相變化材料修整去除，以得到管端鑲埋合金之CNTs。主要的製程參數包括觸媒厚度、氫氣與甲烷比例、氫電漿後處理時間、化學蝕刻時間和熱處理溫度。各個製程步驟的結構與性質分析是以掃描電子顯微技術、穿透電子顯微技術、拉曼光譜技術、歐傑電子頻譜技術以及場發射J-E測量法完成。從此研究中可獲得下列結論。

關於觸媒厚度的影響，較厚的觸媒層可造成CNTs管徑增加和管數密度減少。而對於甲烷濃度的影響，發現在成長CNTs時，較高的碳濃度較傾向沉積破片於其管壁，造成藤蔓狀CNTs而非管狀CNTs的形成。另一方面，成長CNTs時，較高的氫濃度可引起較低的拉曼 I_D/I_G 比，和較多管狀CNTs形成。

氫電漿後處理的基本效用是去除剛成長出之CNTs的頂端碳層，且可能將藤蔓狀CNTs改變成為管狀。氫電漿蝕刻時間可調整至僅蝕刻去除CNTs頂端碳層且依然維持其結構的完整性。換句話說，在7分鐘的氫電漿後處理後，藤蔓狀CNTs可被改變成為沒有頂端碳層覆蓋的管狀CNTs。另一方面，剛成長出的管狀CNTs的頂部碳層可被1分鐘的氫電漿後處理移除，而不會對管身造成過多傷害。此外，氫電漿後處理的優選蝕刻位置是在較大應變區域，例如有較大曲率的位置。而化學蝕刻基本上是藉由化學反應來移除鈷觸媒。目前的情形中，三

分鐘的化學蝕刻幾乎可將所有觸媒從剝離碳層的CNTs頂端去除，使其變為開口端CNTs，且對管身不會造成明顯的傷害。

實驗結果也顯示合金覆蓋的開口端CNTs可在30分鐘420 °C的真空環境熱處理後將相變化合金從他們的側壁調整去除，且變為合金加蓋的CNTs。除此之外，歐傑分析結果顯示在濺鍍製程必須要進行修改，使在碳管頂部被覆蓋相變化材料合金後，可獲得需要的相變化材料的成份。真空高溫下，其成份可能因銻與碲較快的蒸發速率，由富含碲轉變為富含銻的合金。

在場發射的性質上，結果顯示如果CNTs的結構完整性可被維持，因開口端擁有較高的局部深寬比，使得開口端CNTs可能比剛長出之管狀CNTs有較好的場發射性質。另一方面。被剝離頂部碳層的CNTs與剛成長的CNTs作一比較，發現可能因為缺乏碳層的保護，使裸露的觸媒被氧化，造成場發射性質衰退。氫電漿後處理也可能造成更多的缺陷與平坦的表面於管頂，使得場發射性質下降。

**Nanofabrication of the alloy-ended CNTs and the structure-property analyses
at each processing step**

Graduate student: Kuo-Ming Chiu

Professor: Cheng-Tze Kuo

National Chiao Tung University
Department of Material Science & Engineering

Abstract

In order to cap the tip cavities of the open-ended carbon nanotubes (CNTs) with the phase-change alloy for potential applications as the nano-resolution storage media, the Co-assisted CNTs were first synthesized by electron cyclotron resonance chemical vapor deposition (ECR-CVD) with H₂ and CH₄ as the gas sources. Then, the as-grown CNTs were post-treated in H-plasma atmosphere to remove the carbon layers covered on catalysts, and subsequently immersed in 0.25 M HNO₃ solution to remove the catalysts from the tips. The open-ended CNTs with a bowl-like-shape tips were followed by coating with a phase-change alloy layer of Ge₂Sb₂Te₅ (200 nm in thickness) via sputtering process, and then heat treated in vacuum (10⁻³ Torr) for 30 minutes to trim the alloy off from the sidewalls of CNTs to obtain the alloy-ended CNTs. The main processing parameters include catalyst thickness, H₂/CH₄ ratio, time of H-plasma post-treatment, chemical etching time and heat-treating temperature. The structures and properties in each processing step were characterized by scanning electron microscopy (SEM), transmission electron microscopy (TEM), Raman spectroscopy, Auger electron spectroscopy (AES) and field emission J-E measurements. The following conclusions can be drawn from these studies.

Regarding effect of catalyst thickness, a thicker catalyst layer can result in an increase in tube diameter and a decrease in tube number density of CNTs. As to effect of CH₄ concentration, a greater carbon concentration is more favor to grow CNTs with carbon sheets on the sidewalls of CNTs to become the rattan-like CNTs instead of tubule-like CNTs. On the other hand, a higher H₂ concentration during CNTs growth can give rise to a lower Raman I_D/I_G ratio and more tubule-like CNTs formation.

Effect of H-plasma post-treatment is essentially to remove the carbon layers from the

as-grown CNTs tips and may cause the rattan-like CNTs to become tubule-like CNTs. The H-plasma etching time can be varied to merely etch off the carbon layers on the tips of CNTs and still maintain the structure integrity. In other words, the rattan-like CNTs can be changed to the tubule-like CNTs without carbon layers on the tips by 7 min post H-plasma treatment. On the other hand, the carbon layers on the tips of the as-grown tubule-like CNTs can be removed by 1 min H-plasma post-treatment without too much damage to the stems of CNTs. Furthermore, it is found that the preferred etching sites for H-plasma post-treatment are on the higher strained areas, such as regions with the greater curvatures. Effect of chemical etching is basically to remove the Co-catalyst off by chemical reaction. Under the present conditions, 3 min chemical etching time can almost remove all catalysts from the carbon layer-stripped tips to become the open-ended CNTs without significant damage to their stems.

The experimental results also show that the alloy-coated open-ended CNTs can be heat treated to trim off the alloys from their sidewalls in vacuum at 420°C for 30 min to become an alloy-capped CNTs. Furthermore, the Auger analyses show that the sputtering process must be modified to obtain the required composition of phase-change alloy after being capped on the tips of CNTs, where the compositions of the phase-change alloys may be changed from Te-rich to Ge-rich due to the faster evaporation rates of Sb and Te.

Regarding field emission properties, the results indicate that the open-ended CNTs may behave better properties than the as-grown tubule-like CNTs due to higher local aspect ratio around the open-ended tips, if their structure integrity can be maintained. On the other hand, the field emission properties of the carbon layer-stripped CNTs are declined by comparing with the as-grown CNTs due to oxidation of the exposed catalysts without carbon layer protection. H-plasma post-treatment may also cause a decrease in field emission properties by forming more defects and flatten surfaces at the tips.

Acknowledgement

首先十分感謝郭正次教授兩年來的教誨提攜，對於實驗的想法與論文寫作技巧方面的悉心指導，我會謹記在心。也感謝李驊登、林景崎、潘扶民教授等口試委員，百忙之中抽空參與口試過程，對於實驗與論文方面的指教，都使我獲益匪淺。

同時感謝威翔、兆焄、柏林、淑幸、智明、必愷、貞君等學長姐在實驗儀器與實驗過程中給予的建議與幫助。還有陪伴著我一起渡過兩年碩士班生涯的竣愷、奕同、怡芬、土狼、陳德勝、伍泰霖和恰吉，從諸位身上，獲得許多寶貴的知識；在我曾經不開心或實驗上遇到瓶頸的時候，感謝你們的鼓勵與陪伴。在此也要感謝可愛的伊茹、玉蓉、佑君等學弟妹對於實驗上的幫助以及生活上的支持。

時間過得很快，兩年的碩士班生涯已經結束了，這兩年內發生了許多值得回味的事，有甘有苦，曾經共患難、相互扶持的革命情感，相信大家一輩子都不會忘記。還要感謝家人給予的支持，可以讓我在無後顧之憂的情況下，完成這篇碩士論文。還有陪伴我給予我心靈支持的女友茶毓，謝謝妳對我的照顧與在繪圖上的幫忙。謹祝郭正次教授實驗室的各位成員，在往後的研究過程能順利，完成更多更好的研究。

Contents

Chinese abstract	I
English abstract	III
Acknowledgement	V
Contents	VI
List of symbols	IX
Table captions	XI
Figure captions	XII
Chapter 1 introduction	1-1
1.1 Introduction to phase-change storage media.....	1-1
1.2 Introduction to carbon nanotubes (CNTs).....	1-2
1.3 Motivation.....	1-3
Chapter 2 Literature reviews	2-1
2.1 CNTs and their features.....	2-1
2.2 Nanofabrications of the open-ended CNTs.....	2-2
2.2.1 Oxidation method.....	2-2
2.2.2 Plasma etching methods.....	2-3
2.2.3 Chemical etching methods.....	2-4
2.2.4 AAO template-assisted and Ar ⁺ ion milling method.....	2-5
2.3 Properties and potentialities of open-ended CNTs.....	2-6
2.4 Nanofabrications of the material filled CNTs.....	2-7
2.4.1 Material filling during CNTs fabrication.....	2-8
2.4.2 Material filling after CNTs formation.....	2-8
2.5 Storage mechanisms of optical phase-change storage media.....	2-10
2.6 Specifications of the typical rewritable memory media.....	2-11
2.7 Analysis methods.....	2-12

2.7.1 Analyses of CNTs.....	2-12
2.7.2 Analysis methods of phase-change storage media.....	2-12
Tables.....	2-14
Figures.....	2-15
Chapter 3 Experimental methods.....	3-1
3.1 Process description and flow chart.....	3-1
3.2 Raw materials.....	3-1
3.3 ECR-CVD system.....	3-1
3.4 Catalyst deposition and H plasma pretreatment	3-2
3.5 CNTs growth in ECR-CVD.....	3-3
3.6 Post-treatments.....	3-3
3.6.1 H-plasma and chemical etching.....	3-3
3.6.2 Alloy sputtering and high temperature tip trimming	3-4
3.7 Analysis methods.....	3-4
3.7.1 SEM and TEM examinations.....	3-4
3.7.2 Raman and AES analyses.....	3-5
3.7.3 Field emission measurements.....	3-6
Tables.....	3-7
Figures.....	3-8
Chapter 4 Results and discussions.....	4-1
4.1 Effects of catalyst thickness on CNTs growth.....	4-1
4.2 Effects of H ₂ and CH ₄ flow rate on CNTs growth.....	4-1
4.3 H-plasma and chemical etching post treatment for the open-ended CNTs.....	4-2
4.4 Mechanism of H-plasma post-treatment.....	4-3
4.5 Structure and composition variations by high temperature tip trimming.....	4-4
4.6 Raman spectra of CNTs.....	4-5
4.7 CNTs morphology versus field emission property.....	4-5
Tables.....	4-8
Figures.....	4-10
Chapter 5 Conclusions.....	5-1

Figures.....5-3
References.....R1

ZEON PDF Driver Trial
www.zeon.com.tw

The logo is a circular emblem with a gear-like outer border. Inside the circle, there is a stylized blue figure that appears to be a person or a character. The letters 'ES' are prominently displayed in the center of the figure. Below the figure, the year '1896' is written. The entire logo is rendered in a light blue color.

List of symbols

1-D	One-dimension
AES	Auger Electron Spectroscopy
AFM	Atomic Force Microscopy
B	Magnetic field
β	Field amplification factor
C	Reflectivity contrast
C_h	Chiral vector
CNTs	Carbon nanotubes
D.C.	Direct current
DSC	Differential Scanning Calorimetry
DVD	Digital Versatile Disks
e	Electron charge (coulombs)
E	Electronic field
ECR-CVD	Cyclotron Resonance Chemical Vapor Deposition
FED	Field Emission Display
FEM	Field Emission Microscopy
F-N	Fowler-Nordheim
HRTEM	High Resolution Transmission Electron Microscopy
H_v	Heat of vaporization
ϕ	Work function
J	Current density
λ	Wave length
m_e	Mass of electron
MWNTs	Multi-walled carbon nanotubes
r_c	Cyclotron radius
R_f	The reflectivity of the regions after writing
R_i	The reflectivity of the regions before writing
SAED	Selected-Area Electron Diffraction

SEM	Scanning Electron Microscopy
SWNTs	Single-walled carbon nanotubes
TEM	Transmission Electron Microscopy
T_m	Melting point
v	Electron velocity
ω	Electron angular frequency

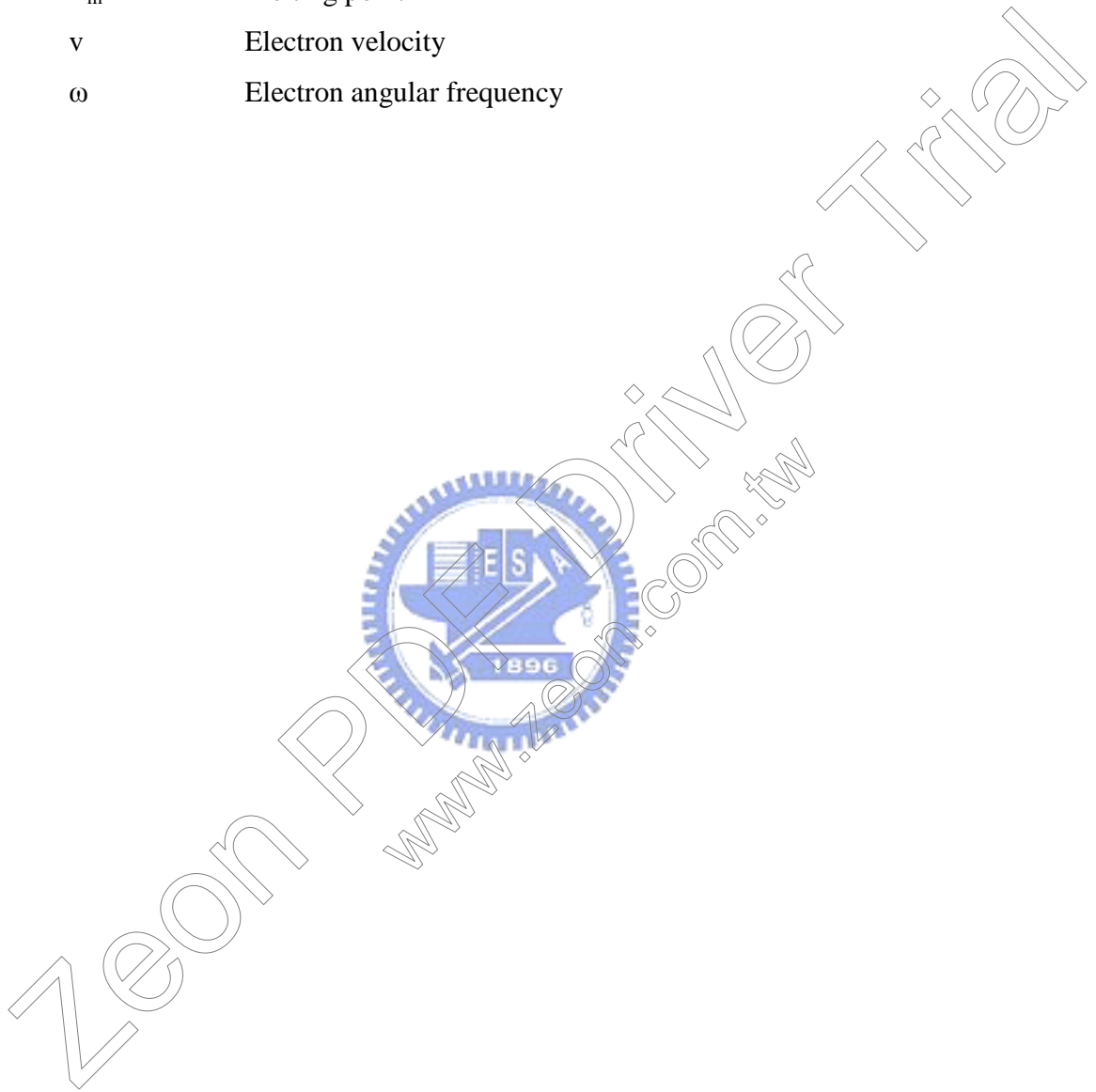
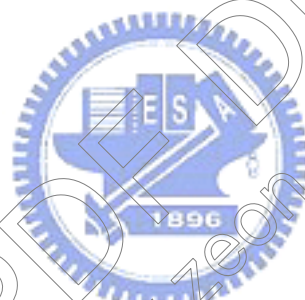


Table captions

Table 2-1	List of phase-change material ^[±. 98-P. 121]	2-14
Table 2-2	Basic physical properties of Ge, Sb, Te and Co ^[http://environmentalchemistry]	2-14
Table 3-1	Specimen designation and processing conditions of CNTs.....	3-7
Table 3-2	H-plasma and chemical etching post-treatment conditions.....	3-7
Table 4-1	Morphologies and bonding structures of various CNTs.....	4-8
Table 4-2	Morphologies of the as-grown and post-treated CNTs.....	4-8
Table 4-3	Field emission properties and features of CNTs for Specimen C1 after different post-treatment conditions.....	4-9



ZEON PDF Driver
www.zeon.com.tw

Figure captions

- Fig. 2-1 Depiction of fullerene and CNTs structure. CNTs can be considered the “elongated” Fullerene ^[Dresselhaus 96-P. 756]2-15
- Figs. 2-2 The possible structure models for a graphitic tubule. (a) Each cylinder represents a coaxial closed layer of carbon hexagons. (b) Helical arrangement of the hexagons ^[Iijima 91-56]2-15
- Figs. 2-3 (a) Graphene tubules are made by rolling a graphene sheet into a cylinder. The tubules are uniquely determined by their lattice vectors \mathbf{c}_k . The chiral angle is denoted by θ , while \mathbf{a}_1 and \mathbf{a}_2 denote the unit vectors of graphite. (b) Possible vectors for chiral fibers. The circled dots and dots, respectively, denote metallic and semiconducting behavior for each Fiber ^[Saito 92-2204]2-16
- Figs. 2-4 (a) Bamboo-like CNTs ^[Lee 00-560]. (b) Y-junction CNTs ^[Li 01-1879]. (c) Helical CNTs ^[郭 04-P. 4-24]. (d) H-junction CNTs ^[Ting 02-324]. (e) Bill-like CNTs ^[郭 04-P. 4-25]2-17
- Fig. 2-5 TEM images of CNTs from a CNT array which was treated by O₂ oxidation for 20 min at 400 °C ^[Kung 02-4819]2-18
- Fig. 2-6 TEM image, the molten Pd particles were drawn into the opened-tips and elongate to form Pd nanorods ^[Tsai 99-3462]2-18
- Figs. 2-7 Schematic of the growth mechanism, (a) nucleation of carbon nanotubes, (b) growth of carbon nanotubes and melting of the Pd nanoparticles, (c) sinking and elongating of the Pd droplet, and (d) opening of the carbon nanotubes and formation of the Pd nanorod ^[Tsai 99-3462]2-19
- Figs. 2-8 A comparison of TEM bright-field image between conventional and a layer-by-layer deposited CNTs; (a) conventional CNTs (b) end point ^[Chung 01-73]2-19
- Figs. 2-9 Transmission electron microscopy images of (a) the curly and closed MWNTs grown in CH₄ and H₂ plasma by the PECVD method, (b) the aligned and open MWNTs grown using CH₄, H₂, and O₂ reaction gas ^[Lee 02-577]2-20
- Figs. 2-10 SEM images of an aligned nanotube film before and after H₂O-plasma etching (a) a large area aligned nanotube film covered by a thin amorphous carbon layer on a quartz glass plate before plasma treatment, (b) the same nanotube film as (a) after the H₂O-plasma etching for 30 min at 250 kHz, 30 W, and 0.62 Torr. Note that the micrographs shown in (a) and (b) were not taken from the same spot due to technical difficulties ^[Huang 02-3549]2-20

Fig. 2-11	SEM images of the aligned nanotubes after the plasma-treatment for 80 min, followed by a gentle wash with HCl (37%) to remove the Fe catalyst residues ^[Huang 02-3549]	2-21
Figs. 2-12	TEM images(a) NTs with different diameters initially grown on the steel surface. (b) Open-end NTs produced by electrochemical etching ^[Wang 01-4028]	2-21
Figs. 2-13	Typical high-resolution electron micrographs of nitric acid treated nanotubes. (a) Attack has occurred at point X and Y where non-six-membered Carbon ring are represent. (b) and (c), Arrows show site of the destruction of multiple internal caps by nitrite acid treatment. Scale bar, 50Å ^[Tsang 94-159]	2-22
Figs. 2-14	Schematics of fabrication of the open and closed tip CNTs using AAO templates. The processes correspond to (a) fabrication of CNTs, (b) and (c) ion millings, and (d) etching in acid solution ^[Yoon 04-825]	2-22
Figs. 2-15	SEM images of the closed (a), (c) and open (b), (d) tips of CNTs fabricated on AAO templates. The height of the tips could be controlled by changing the etching time in acid solution and its deviation was about 2 nm ^[Yoon 04-825]	2-23
Figs. 2-16	(a) AFM image, (b) MFM image and (c) the corresponding MFM line scan profile for Fe catalyst-assisted CNTs, respectively ^[Kuo 03-799]	2-23
Figs. 2-17	High-resolution TEM images of tubes filled (darker contrast in the centre) with vanadium oxide. (a) Filling in a narrow internal hollow, showing amorphous structure. (b) Crystalline V ₂ O ₅ structure in a larger hallow (only 2~3 tube layers around the filling is shown) showing preferred orientation with respect to the tube axis ^[Ajayan 95-564]	2-24
Figs. 2-18	TEM images of the opened carbon nanotubes (a) before and (b) after filling with the Ag nanorod. Note that the micrographs shown in (a) and (b) were not taken from the same nanotubes due to technical difficulties ^[Huang 02-3543]	2-24
Fig. 2-19	High resolution electron micrograph of a nickel material filled nanotubes also opened at point X and Y; the observed fringes of 2.40 0.05 Å correspond to (111) NiO crystal plane. Scale bar, 50 Å ^[Tsang 94-159]	2-24
Fig. 2-20	GeTe-Sb ₂ Te ₃ pseudobinary phase diagram and phase transition temperatures of GeTe-Sb, Te, pseudobinary amorphous alloy films ^[Yamada 91-2849]	2-25
Fig. 2-21	DSC curves for the GeTe-Sb ₂ Te ₃ psedobinary system at heating rate of 10 deg/min ^[Yamada 91-2849]	2-25
Fig. 3-1	Flow chart of this experiment.	3-8
Fig. 3-2	Schematic diagram of ECR-CVD system.	3-9

Figs. 4-1	Effect of H ₂ /CH ₄ ratio (sccm/sccm) and catalyst thickness on CNTs morphology. (a), (b) and (c) are 100 nm Co-assisted CNTs grown with H ₂ /CH ₄ ratio = 10/20, 10/10 and 20/10, respectively. (d), (e) and (f) are 150 nm Co-assisted CNTs grown with H ₂ /CH ₄ ratio = 10/20, 10/10 and 20/10, respectively.....	4-10
Figs. 4-2	The corresponding side view SEM images of Figs. 4-1.....	4-11
Figs. 4-3	Effect of H-plasma post-treatment on rattan-like CNTs morphology. (a), (b) and (c) are the top view SEM images of CNTs H-plasma post-treated for 1, 4 and 7 min (Con. 1, 4 and 5), respectively. (d), (e) and (f) are the corresponding side view of (a), (b) and (c), respectively.....	4-12
Figs. 4-4	Effect of H-plasma post-treatment and chemical etching on rattan-like CNTs morphology. (a) and (b) are the top view and side view SEM images of rattan-like CNTs post-treated by 7 min H-plasma etching and followed by 3 min chemical etching (Con. 6), respectively.....	4-13
Figs. 4-5	(a) TEM and (b) SEM micrographs of as-grown CNTs with tip carbon layer (Specimen C1). Arrows mark the strained regions with largest curvature.....	4-14
Figs. 4-6	The SEM morphologies of the CNTs after different H-plasma post-treatment times: (a) 1 min (Con. 1), (b) 4 min (Con. 4), (c) 7 min (Con. 5) and (d) 10 min (Con.7). (Specimen C1).....	4-15
Fig. 4-7	TEM image of CNTs etched by H plasma for 1 min (Specimen C1, Con. 1). Carbon layers have been removed. Arrows mark the preferred etched region.....	4-16
Fig. 4-8	TEM image of the CNTs etched by H plasma for 10 min (Specimen C1, Con. 7).....	4-16
Figs. 4-9	SEM morphologies of post-treated CNTs for Specimen C1 (a) H plasma etched for 1 min and chemical etched for 2 min (Con. 2), (b) H plasma etched for 1 min and chemical etched for 3 min (Con. 3).....	4-17
Figs. 4-10	Effect of chemical etching time on the catalyst. (a) and (b) are the corresponding TEM micrographs of Fig. 4-9 (a) and (b), respectively.....	4-18
Figs. 4-11	SEM images of open-ended CNTs covered 200 nm phase-change alloy (a) as-alloy-sputtered CNTs, (b) after 400°C heating for 30 min, (c) after 420°C heating for 30 min and (d) after 440°C heating for 30 min.....	4-19
Fig. 4-12	The corresponding TEM micrograph of Fig. 4-11 (b).....	4-20
Fig. 4-13	The corresponding TEM micrograph of Fig. 4-11 (c).The upper right insert showed the selected-area electron diffraction (SAED) pattern of the residual phase-change	

	alloy on CNTs tip.....	4-20
Fig. 4-14	The corresponding TEM micrograph of Fig. 4-11 (d).....	4-21
Fig. 4-15	The Upper and under Auger spectra represent residual phase-change alloy on tips of open-ended CNTs covered 200 nm phase-change alloy post-treated by 400°C heating for 30 min and 420°C heating for 30 min, respectively.....	4-21
Figs. 4-16	Raman spectra of 100 nm Co-assisted CNTs grown with different H ₂ /CH ₄ ratio (sccm/sccm) (a) 10/20 (b) 10/10 (c) 20/10.....	4-22
Figs. 4-17	Raman spectra of 150 nm Co-assisted CNTs grown with different H ₂ /CH ₄ ratio (sccm/sccm) (a) 10/20 (b) 10/10 (c) 20/10.....	4-23
Figs. 4-18	(a) J-E curves of the as-grown CNTs (Curve 1) and CNTs post-treated by 1 min H-plasma etching (Curve 2), 1 min H-plasma etching + 3 min chemical etching (Curve 3) and 10 min H-plasma etching (Curve 4). (b) The corresponding F-N plots of (a). (Specimen C1).....	4-24
Figs. 5-1	My proposed mechanism of CNTs morphology in each process. (a) As-grown CNTs. (b) H plasma treated CNTs. (c) HNO ₃ solution treated CNTs. (d) Open-ended CNTs covered phase-change alloy. (e) Heat treated CNTs.....	5-3